Electrochemical experimental analysis of different coatings

.

ABSTRACT

Aims: In this paper, for the working condition of turbine final blades, four different metal coatings based on 17-4PH stainless steel are investigated to simulate the working condition of turbine blades, and electrochemical tests are carried out on the four different specimens in the test solution of synthesized seawater solution.
Study design: The self-corrosion current densities of the different specimens in the synthetic seawater solution were measured by means of open circuit, polarization curves and electrochemical AC impedance spectra.
Place and Duration of Study: Department Between July 10, 2023 and August 10, 2023, the Laboratory of the School of Mechanics, North China University of Water Resources and Hydropower (NUWRH).
Methodology: For the working condition of turbine final blades, four different metal coatings based on 17-4PH stainless steel are investigated to simulate the working condition of turbine blades, and electrochemical tests are carried out on the four different specimens in the test solution of synthesized seawater solution. The self-corrosion current densities of the different specimens in the synthetic seawater solution were measured by means of open circuit, polarization curves and electrochemical AC impedance spectra.
Results: The results show that the AHP-coated 17- 4PH stainless steel specimens have the lowest self-corrosion current density (icorr) in the synthetic seawater solution.
Conclusion: Non-invasive This indicates that the corrosion rate of AHP coatings in synthetic seawater solutions is slower than that of TW-7 coatings, sprayed stainless steels, and other stainless steels in the same conditions.

Keywords: metal coating; electrochemistry; synthetic seawater; corrosion resistance

1. INTRODUCTION

With the continuous development of economic globalization, mankind's exploration and research in the marine field has reached an unprecedented level[1]. Our country also follows the trend of the times, and with it comes the development and utilization of marine resources, which not only brings abundant resources to our country, but also further gives full play to our marine development strategy, ensures the security of our marine territories[2], and pushes forward the construction and development of a strong country based on the sea. Most of the equipment currently in use is based on metal, so when metal equipment is exposed to harsh environments for a long period of time, it will inevitably suffer from different degrees of wear and corrosion[3]. One of the most effective ways to improve the corrosion resistance of metals is to treat the substrate[4]. One of the most important and effective

methods of surface treatment is to protect the surface of the substrate with a coating layer[5]. In recent years, scientists at home and abroad have carried out a lot of research and experiments on the corrosion and protection of metals[6]. Up to now, the current methods of corrosion protection of metals include: coating protection, changing the structure of the metal, electrochemical protection, surface treatment of the metal, media treatment, corrosion inhibitor protection, temperature protection and maintenance[7]. Individually or in combination, these methods can provide effective protection against corrosion and thus reduce the risk to the metal, but in practice the most suitable method of protection should be selected on a case-by-case basis. In the present review, the main focus of this paper is to analyze the feasibility of electrochemical protection of metal coatings used for the protection of turbine upper stage blades by simulating electrochemical tests in a synthetic seawater environment[8].

2. MATERIAL AND METHODS

The material used in the experiment is steel[9]. 17-4PH stainless steel is a commonly used low carbon steel, the yield strength is generally between 725-1180MPa, with high strength and corrosion resistance, good welding performance and processing performance, widely used in construction, machinery manufacturing, highways and bridges, etc[10].And its chemical composition contains carbon, silicon and manganese,Sulfur, phosphorus, etc[11].The specific composition is shown in Table 1.

Table 1. Composition of experimental materials (%)

C	Si	Mn	S	P	(sth. or sb) else
≤0.22	≤0.35	≤1.40	≤0.045	≤0.045	Fe

The TW-7 coatings, AHP coatings and sandblasted SERMETEL coatings are produced by applying a high temperature resistant topcoat consisting of silicone, high temperature resistant pigmented fillers, additives and organic solvents. Main Properties: Good heat resistance up to 200°C for a long period of time; good adhesion; moisture resistance,Oil-resistant performance; good weather resistance; can be directly constructed on high temperature substrates at 200℃. Used in boilers[12].It is used on steel surfaces where the temperature of engine casing, exhaust pipe, chimney, oven and other high-temperature equipments and pipelines is less than 200℃[13]. According to the technical standard of inorganic phosphate coating layer, the production process is based on 17-4PH stainless steel[14].

Material leakage in the ambient temperature of 20-40 ℃, its relative humidity control for 40% -70%. Detailed operation is as follows:

(1) Sandblasting. Test forged samples with 40 mesh white corundum sand, sandblast the samples, and then use compressed air to blow away the dust on the outside of the substrate and abrade the material at the same time. When sandblasting a flat surface, make sure that the spraying angle is about 65°~75°, and keep a distance of 250-280mm between the nozzle and the workpiece when spraying at right angles.

Distance. The process should keep the environment clean to avoid contamination[15].

(2) Bottom slurry mixing and spraying. Adopt mechanical mixer to mix the slurry for three hours, filter and remove impurities with 150-mesh filter to ensure that the slurry is uniform and non-layered, as well as precipitation and shelf-life slurry[16]. Spraying two times in total to

ensure that the spraying is sufficient and the interval between each spraying is 20 minutes to ensure that the specimen is completely dry before proceeding.
Spraying.
(3) Curing and shot peening of the substrate base. After spraying, the samples are cured in a heat treatment oven[17]. The performance parameters were: hold at 200°C for 70 minutes, then heat to 380°C and hold for 70 minutes. The air in the furnace was cooled to room temperature[18]. Spray the bottom layer with granules after curing using a spray pressure of 0.4-0.5 MPa. At the same time turn on the compressed air and release it for 10-15 minutes. Check the surface for compressed air[19].External and shot peening can only be carried out in the absence of water.
(4) Coatings are sprayed and cured. Hold at 100°C for 50 min, then increase the temperature to 400°C for 50 min and cool to room temperature in a heat treatment oven. The curing procedure was repeated. In total, two coats were applied[20].
Make sure that the spraying is sufficient and that the interval between each spraying is 20 minutes to ensure that the specimen is completely dry before spraying.
The instrument used in this experiment is an electrochemical workstation as shown in figure 1.

Fig. 1.Electrochemical Workstation

In this experiment, four different coatings were tested on an electrochemical workstation with a synthetic seawater solution at 23±2°C as the electrolyte, using a three-electrode system with saturated calomel as the reference electrode, platinum sheet as the counter electrode, and the sample as the working electrode. The open-circuit potential was used as the measurement potential, and the impedance response characteristics were tested in the frequency range of 0.01-100 kHz. The polarization curves were measured in the potential range of ±0.5 V open-circuit potential, and the scanning rate of 0.5 mV was used to compare the electrochemical impedance response of the coatings before and after the experiments.

2.1 Electrochemical experiment results and analysis

Figure 2 shows the open-circuit potentials of the four samples in synthetic seawater, with values ranging from -0.77V to -0.67V. The sandblasted SERMETEL coating sample has the largest open-circuit potential, while the TW-7 sample has the smallest open-circuit potential. The composition of the synthesized seawater is shown in Table 2.

Table 2. Synthetic seawater components and their concentrations

individual parts making up a compound	common salt	magnesium chloride	magnesium sulfate	calcium chloride	dicalcium phosphate	sodium bicarbonate	sodium bromide
concentration	26.5g/L	2.4g/L	3.3 g/L	1.1 g/L	0.73 g/L	0.2 g/L	0.28 g/L

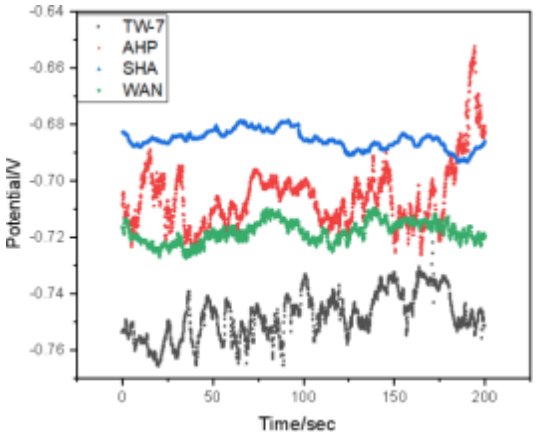

Fig.2.Open-circuit potentials of four specimens in synthetic seawater

Figure 3 shows the polarization curves of the four specimens, in which it can be seen that the four specimens have more obvious passivation characteristics. Table 3 is the self-corrosion potential and self-corrosion current density obtained by fitting the polarization curves. The level of self-corrosion potential represents the ease of corrosion, the higher the self-corrosion potential is, the less likely that galvanic corrosion will occur, and the lower it is, the more likely that galvanic corrosion will occur. the AHP coating has the highest self-corrosion potential and the lowest self-corrosion potential at the same time, which indicates that the AHP coating is the least prone to galvanic corrosion, and once corrosion occurs, the corrosion rate is lower than the rest of the specimens. The sandblasted specimens have the lowest self-corrosion potential and the highest self-corrosion potentialof the self-corrosion current density, which indicates that the sandblasted specimen has the worst corrosion resistance among these four specimens.

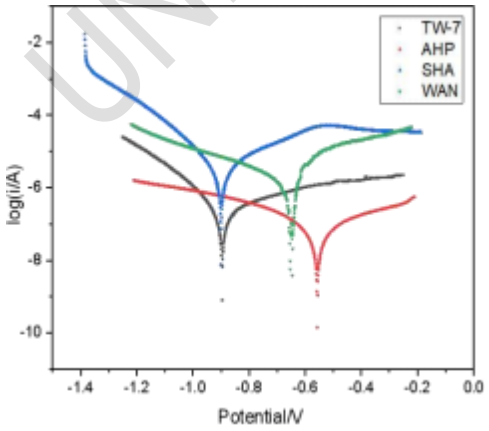

Fig.3.Polarization curves of four specimens in synthetic seawater

Table 3. Polarization curve fit data

Specimen number	Self-corrosion potential Ecorr (V)	Self-corrosion current density icorr (A/cm2)
TW-7	-0.895	2.225 x 10-7
AHP	-0.557	5.961 x 10-8
Sandblasted SERMETEL coatings	-0.900	3.169 x 10-6
Shot Peening SERMETEL Coatings	-0.646	3.989 x 10-7

Figure 4 shows the Bode and Nyquist plots of the AC impedance of the four specimens, respectively. Because of the poor conductivity of the inorganic phosphate coatings, the impedance spectra are scattered at low frequencies, and the AC impedance was fitted to an R(CR) type circuit. The fitted data are shown in Table 4. The AHP coating has the largest polarization resistance value, which is consistent with the polarization curve results.

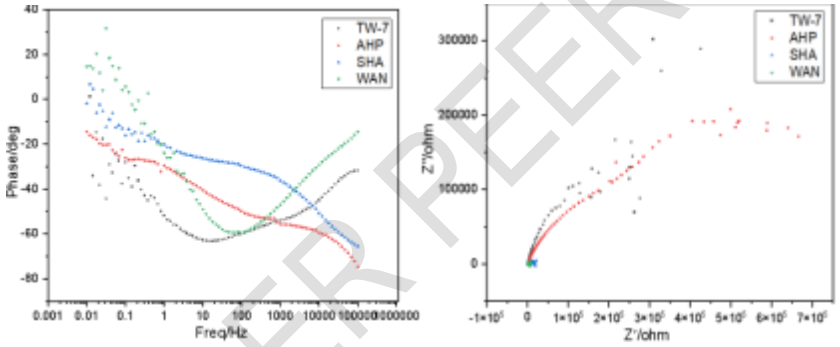

Fig.4.AC impedance spectra (Bode plot) and AC impedance spectra (Nyquist plot) of four specimens in synthetic seawater solution

Table 4. AC impedance fitting data

Specimen number	Rs	C	Rp
TW-7	301.4	4.021 x 10-7	3.706×105
AHP	1424	2.941 x 10-8	4.536 x 105
Sandblasted SERMETEL coatings	1271	1.353 x 10-6	1.16 x 104
Shot Peening SERMETEL Coatings	56.89	2.362 x 10-6	6.646 x 103

3. CONCLUSION

The AHP-coated 17-4PH stainless steel samples all have the lowest self-corrosion current density (icorr) in synthetic seawater solutions, which indicates that AHP coatings corrode slower in synthetic seawater solutions than TW-7, shot peened SERMETEL, and sandblasted SERMETEL in the same conditionsLayer.

CONSENT (WHEREEVER APPLICABLE)

All authors declare that 'written informed consent was obtained from the patient (or other approved parties) for publication of this case report and accompanying images. A copy of the written consent is available for review by the Editorial office/Chief Editor/Editorial Board members of this journal.

ETHICAL APPROVAL (WHEREEVER APPLICABLE)

All authors hereby declare that all experiments have been examined and approved by the appropriate ethics committee and have therefore been performed in accordance with the ethical standards laid down in the 1964 Declaration of Helsinki.

REFERENCES

1. B.I. S S, ALEXANDRO R-R, JENS R, et al. Biocides used as material preservatives mo dify rates of de novo mutation and horizontal gene transfer in bacteria. 2022, 437: 1292 80-.
2. TANG Z, GAO J, XU Z, et al. Effect of Laser Shock Peening on the Fatigue Life of 1Cr1 2Ni3Mo2VN Steel for Steam Turbine Blades. 2023, 13(9).
3. GUAN J, LV X, WENG Y. A dual-driven approach for refined modeling and performanc e analysis of heavy-duty gas turbine. 2024, 244: 122710-.
4. Xiamen University; Researchers Submit Patent Application, "Method For Anti-Corrosion Treatment Of Metallic Copper-Containing Materials", for Approval (USPTO 202002243 20). 2020.
5. LIU P, YUAN X, HAN Q, et al. Micro-defect Varifocal Network: Channel attention and sp atial feature fusion for turbine blade surface micro-defect detection. 2024, 133(PA): 108 075-.
6. YANG S, GAO S, XUE W, et al. Oxidation and hot corrosion behaviors of NiAlTa protec tive material for turbine single crystal blade tips. 2024, 230: 111899-.
7. SIHOMBING S, NABABAN W S, SIAGIAN P, et al. Influence of induction motorcycle in electricity generator which involved stated turbine protection reviewed by characteristic vibration and time domain. 2018, 420(1).
8. SOUHIR T. Optimal design and control of hybrid synchronous generator regulating turbi ne angular speed for turbine protection. 2023, 47(5): 1033-47.
9. SHI L, CHEN D, QI T. Analysis of SEIMENS Class F Gas Turbine Protection System, F, 2016.

10. HU P, MENG Q, FAN W, et al. Vibration characteristics and life prediction of last stage blade in steam turbine Based on wet steam model. 2024, 159: 108127-.

11. BALASO F B, JAGTAP H P. Failure analysis steam turbine in sugar factory thermal po wer plant: a Review. 2024, 1285(1).

12. ARTYUKHOV D I, I A D, F S S, et al. Use of photovoltaic converters in electrochemical protection systems for underground pipelines. 2020, 1652(1): 012030-.

13. XIAOQI Z, BAOMIN F, NING Q, et al. Stabilized Ti3C2Tx-doped 3D vesicle polypyrrole coating for efficient protection toward copper in artificial seawater. 2024, 642.

14. REDONDO F L, VILLAR M A, CIOLINO A E, et al. Development and characterisation of block copolymer/bioactive glass and block copolymer/TCP composite coatings obtaine d by EPD. 2024, 362: 136159-.

15. BAO P, LI H, CHEN Y, et al. The GO composite coatings for enhancing interfacial inter action performance and desensitization of CL-20. 2024, 316: 128968-.

16. HASAN J A, HUSEIN K S M, KAMIL A S, et al. The effective and sustainable applicatio n of a green amino acid-based corrosion Inhibitor for Cu metal. 2023, 7: 100316-.

17. R. A D, YA. V M, A. I G, et al. Guanidine-Containing Alkyl-Substituted Oligomer as a M etal Corrosion Inhibitor. 2023, 58(5): 579-84.

18. ABOU E A, M. M E, F. S D, et al. Recyclization of Expired Megavit Zinc (MZ) Drug as M etallic Corrosion Inhibitor for Copper Alloy C10100 in Nitric Acid Solution. 2021, 7(2).

19. VAHID A, CHANGIZ D. The effect of grain size on the corrosion inhibitor adsorption of nanocrystalline iron metal. 2010, 101(3): 366-71.

20. Li Wei, Li Taijiang, Wang Shaodong, et al. Experimental Study on Repairing and Protec ting Water Corrosion Damage of Turbine Final Stage Dynamic Blade. 2011, 40(01): 40-4.Chinese.